T1000: A reduced gene set prioritized for toxicogenomic studies

Othman Soufan [1] , **Jessica Ewald** [2] , **Charles Viau** [1] , **Doug Crump** [3] , **Markus Hecker** [4] , **Niladri Basu** [Corresp., 2] , **Jianguo Xia** [Corresp. 5, 6]

[1] Institute of Parasitology, McGill University, Montreal, Canada

[2] Faculty of Agricultural and Environmental Sciences, McGill University, Montreal, Canada

[3] Ecotoxicology and Wildlife Health Division, Environment and Climate Change Canada, National Wildlife Research Centre, Carleton University, Ottawa, Canada

[4] School of the Environment & Sustainability and Toxicology Centre, University of Saskatchewan, Saskatoon, Canada

[5] Institute of Parasitology, McGill University, Montreal, Quebec, Canada

[6] Department of Animal Science, McGill University, Montreal, Quebec, Canada

Corresponding Authors: Niladri Basu, Jianguo Xia
Email address: niladri.basu@mcgill.ca, jeff.xia@mcgill.ca

There is growing interest within regulatory agencies and toxicological research communities to develop, test, and apply new approaches, such as toxicogenomics, to more efficiently evaluate chemical hazards. Given the complexity of analyzing thousands of genes simultaneously, there is a need to identify reduced gene sets. Though several gene sets have been defined for toxicological applications, few of these were purposefully derived using toxicogenomics data. Here, we developed and applied a systematic approach to identify 1000 genes (called Toxicogenomics-1000 or T1000) highly responsive to chemical exposures. First, a co-expression network of 11,210 genes was built by leveraging microarray data from the Open TG-GATEs program. This network was then re-weighted based on prior knowledge of their biological (KEGG, MSigDB) and toxicological (CTD) relevance. Finally, weighted correlation network analysis was applied to identify 258 gene clusters. T1000 was defined by selecting genes from each cluster that were most associated with outcome measures. For model evaluation, we compared the performance of T1000 to that of other gene sets (L1000, S1500, Genes selected by Limma, and random set) using two external datasets based on the rat model. Additionally, a smaller (T384) and a larger version (T1500) of T1000 were used for dose-response modeling to test the effect of gene set size. Our findings demonstrated that the T1000 gene set is predictive of apical outcomes across a range of conditions (e.g., *in vitro* and *in vivo*, dose-response, multiple species, tissues, and chemicals), and generally performs as well, or better than other gene sets available.

T1000: A reduced gene set prioritized for toxicogenomic studies

[1]Othman Soufan, [2]Jessica Ewald, [1]Charles Viau, [3]Doug Crump, [4]Markus Hecker, [2,*]Niladri Basu and [1,5,*]Jianguo Xia

[1]Institute of Parasitology, McGill University, Montreal, Quebec, Canada; [2]Faculty of Agricultural and Environmental Sciences, McGill University, Montreal, Quebec, Canada; [3]Ecotoxicology and Wildlife Health Division, Environment and Climate Change Canada, National Wildlife Research Centre, Carleton University, Ottawa, Canada; [4]School of the Environment & Sustainability and Toxicology Centre, University of Saskatchewan, Saskatoon, Canada; [5]Department of Animal Science, McGill University, Montreal, Quebec, Canada.

*Correspondance: Niladri Basu

Email: niladri.basu@mcgill.ca

Tel: (514) 398-8642

Address: CINE Building,
21111 Lakeshore Road
Ste. Anne de Bellevue
QC, Canada
H9X 3V9.

*Correspondence: Jianguo Xia

Email: jeff.xia@mcgill.ca

Tel: (514) 398-8668

Address: Office P107, Parasitology Building,
21111 Lakeshore Road
Ste. Anne de Bellevue
QC, Canada
H9X 3V9.

Abstract

There is growing interest within regulatory agencies and toxicological research communities to develop, test, and apply new approaches, such as toxicogenomics, to more efficiently evaluate chemical hazards. Given the complexity of analyzing thousands of genes simultaneously, there is a need to identify reduced gene sets. Though several gene sets have been defined for toxicological applications, few of these were purposefully derived using toxicogenomics data. Here, we developed and applied a systematic approach to identify 1000 genes (called Toxicogenomics-1000 or T1000) highly responsive to chemical exposures. First, a co-expression network of 11,210 genes was built by leveraging microarray data from the Open TG-GATEs program. This network was then re-weighted based on prior knowledge of their biological (KEGG, MSigDB) and toxicological (CTD) relevance. Finally, weighted correlation network analysis was applied to identify 258 gene clusters. T1000 was defined by selecting genes from each cluster that were most associated with outcome measures. For model evaluation, we compared the performance of T1000 to that of other gene sets (L1000, S1500, Genes selected by Limma, and random set) using two external datasets based on the rat model. Additionally, a smaller (T384) and a larger version (T1500) of T1000 were used for dose-response modeling to test the effect of gene set size. Our findings demonstrated that the T1000 gene set is predictive of apical outcomes across a range of conditions (e.g., *in vitro* and *in vivo*, dose-response, multiple species, tissues, and chemicals), and generally performs as well, or better than other gene sets available.

Introduction

Over the past decade there have been profound steps taken across the toxicological sciences and regulatory communities to help transform conventional toxicity testing largely based on animal models and apical outcome measurements to an approach that is founded on systems biology and predictive science (Kavlock et al. 2018; Knudsen et al. 2015; Villeneuve & Garcia-Reyero 2011). On the scientific side, efforts are being exemplified by emergent notions such as the Adverse Outcome Pathway framework (AOP; Ankley et al., 2010) and New Approach Methods (ECHA 2016). On the regulatory side, these are exemplified by changes to, for example, chemical management plans in Canada, the United States and REACH (ECHA 2007) across the European Union.

A core tenet underlying the aforementioned transformations, as catalyzed by the 2007 U.S. National Research Council report “Toxicity Testing in the 21st Century” (Andersen & Krewski 2009), is that perturbations at the molecular-level can be predictive of those at the whole organism-level. Though whole transcriptome profiling is increasingly popular, it still remains costly for routine research and regulatory applications. Additionally, building predictive models with thousands of features introduces problems due to the high dimensionality of the data and so considering a smaller number of genes has the potential to increase classification performance (Alshahrani et al. 2017; Soufan et al. 2015b). Identifying smaller panels of key genes that can be measured, analyzed and interpreted conveniently remain an appealing option for toxicological studies and decision making

In recent years, several initiatives across the life sciences have started to identify reduced gene sets from whole transcriptomic studies. For example, the Library of Integrated Network-Based Cellular Signatures (LINCS) project derived L1000, which is a gene set of 976 'Landmark' genes chosen to infer the expression of 12,031 other highly connected genes in the human transcriptome (Subramanian et al. 2017). In the toxicological sciences, the U.S. Tox21 Program recently published S1500+, which is a set of 2,753 genes designed to be both representative of the whole-transcriptome, while maintaining a minimum coverage of all biological pathways in Kyoto Encyclopedia of Genes and Genomes (KEGG) (Kanehisa et al. 2007) and Molecular Signatures Database (MSigDB) (Liberzon et al. 2015a). The first 1,500 genes were selected by analyzing microarray data from 3,339 different studies, and the rest were nominated by members of the scientific community (Mav et al. 2018). L1000 and S1500 gene sets were originally proposed to serve a different purpose. The 978 landmark genes of L1000 are chosen to infer expression of other genes more accurately, while genes of S1500 are selected to achieve more biological pathway coverage. Compared to L1000, the S1500 gene set attains more toxicological relevance through the gene nomination phase, though its data-driven approach relies upon microarray data primarily derived from non-toxicological studies. It worth nothing that about 33.7% of genes are shared between both signatures. Even though some differences can be realized between L1000 and S1500, they are both strong candidates of gene expression modeling and prediction (Haider et al. 2018).

The objectives of the current study were to develop and apply a systematic approach to identify highly-responsive genes from toxicogenomic studies, and from these to nominate a set of 1000 genes to form the basis for the T1000 (Toxicogenomics-1000) reference gene set. Co-expression network analysis is an established approach using pairwise correlation between genes and clustering methods to group genes with similar expression patterns (van Dam et al. 2018). First, a co-expression network was derived using *in vitro* and *in vivo* data from human and rat studies from the Toxicogenomics Project-Genomics Assisted Toxicity Evaluation System (Open TG-GATEs) database. Next, the connections within the co-expression network were adjusted to increase the focus on genes in KEGG pathways, the MSigDB, or the Comparative Toxicogenomics Database (CTD) (Davis et al. 2017). This incorporation of prior biological and toxicological knowledge was motivated by loose Bayesian inference to refine the computationally-prioritized transcriptomic space. Clusters of highly connected genes were identified from the resulting co-expression network, and machine learning models were applied to prioritize clusters based on their association with apical endpoints. Clustering genes based on expression data has been shown to be instrumental in functional annotation and sample classification (Necsulea et al. 2014), with the rationale that genes with similar expression patterns are likely to participate in the same biological pathways (Budinska et al. 2013). From each cluster key genes were identified for inclusion in T1000. Testing and validation of T1000 was realized through two separate datasets (one from Open TG-GATEs and one from the U.S. National Toxicology Program) that were not used for gene selection. The current study is part of the larger EcoToxChip project (Basu et al. 2019). For the processed data, user can download all samples processed from https://zenodo.org/record/3359047#.XUcTwpMzZ24. We also deposited source codes and scripts used for the study at https://github.com/ecotoxxplorer/t1000.

Materials & Methods

Databases and datasets preparation

The derivation of T1000 was based on five public microarray datasets of toxicological relevance (**Table 1**): four datasets from Open TG-GATEs (Igarashi et al. 2014b), and one dataset generated by Thomas *et al* (referred to as the dose-response dataset in this manuscript; GSE45892) (Thomas et al. 2013). **Table 1** provides a summary of all microarray datasets used in this study. For building the initial T1000 gene set, we used three of the four Open TG-GATEs datasets (see datasets 1-3 in **Table 1**).

Open TG-GATEs

Open TG-GATEs is one of the largest publicly accessible toxicogenomics resources (Igarashi et al. 2014b). This database comprises data from 170 compounds (mostly drugs) with the aim of improving and enhancing drug safety assessment. It contains gene expression profiles and traditional toxicological data derived from *in vivo* (rat) and *in vitro* (primary rat hepatocytes and primary human hepatocytes) studies. To process the raw gene expression data files of Open TG-GATEs, the Affy package (Gautier et al. 2004) was used to produce Robust Multi-array Average (RMA) probe set intensities (Irizarry et al. 2003b). Gene annotation for human and rat was performed using Affymetrix Human Genome U133 Plus 2.0 Array annotation data and Affymetrix Rat Genome 230 2.0 Array annotation data, respectively. Genes without annotation were excluded. When the same gene was mapped multiple times, the average value was used. Finally, all profiles for each type of experiment were joined into a single matrix for downstream analysis.

From the training datasets, specific samples were labelled binary as “dysregulated” or “non-dysregulated”. Dysregulated refers to exposure cases with potential toxic outcomes and non-dysregulated included controls and exposures with non-toxic outcomes. For the *in vitro* datasets, gene expression changes were associated with lactate dehydrogenase (LDH) activity (%). The activity of LDH, which serves as a proxy for cellular injury or dysregulation, was binarized such that values above 105% and below 95% were considered “dysregulated”. While conservative, we note that these cut-off values were situated around the 5% and 95% marks of the LDH distribution curve (see **Supplemental Figure S1** and **Supplemental Information S1** for more details).

For the *in vivo* datasets (kidney and liver datasets from Open TG-GATEs), gene expression changes were associated with histopathological measures. The magnitude of pathologies was previously annotated into an ordinal scale: present, minimal, slight, moderate and severe (Igarashi et al. 2014a). This scale was further reduced into a binary classification with the first three levels considered “non-dysregulated” while the latter two were considered “dysregulated”.

Dose-response dataset and benchmark dose (BMD) calculation

The dose-response dataset (Accession No. GSE45892), was used to externally evaluate the ability of T1000 genes to predict apical endpoints (Thomas et al. 2013). Briefly, this dataset contains Affymetrix HT Rat230 PM microarray data following *in vivo* exposure of rats to six chemicals (TRBZ: 1,2,4-tribromobenzene, BRBZ: bromobenzene, TTCP: 2,3,4,6-tetrachlorophenol, MDMB: 4,4’-methylenebis(*N,N’*-dimethyl)aniline, NDPA: N-nitrosodiphenylamine, and HZBZ: hydrazobenzene). In exposed animals, both gene expression and apical outcomes (liver: absolute liver weight, vacuolation, hypertrophy, microvesiculation, necrosis; thyroid: absolute thyroid weight, follicular cell hypertrophy, follicular cell hyperplasia; bladder: absolute bladder weight, increased mitosis, diffuse transitional epithelial hyperplasia, increased necrosis epithelial cell) were measured, permitting the comparison of transcriptionally-derived benchmark doses (BMD_t) with traditional benchmark doses derived from apical outcomes (Yang et al. 2007). The apical outcome-derived benchmark dose (BMD_a) for each treatment group was defined as the benchmark dose from the most sensitive apical outcome for the given chemical-duration group.

Raw gene expression data (CEL files) for the dose-response dataset were downloaded from GEO (Accession No. GSE45892), organized into chemical-exposure-duration treatment groups, and normalized using the RMA method (Irizarry et al. 2003a). Only expression measurements corresponding to genes in the T1000 gene (or T384 and T1500) set were retained, resulting in reduced gene expression matrices for each treatment group ($t = 24$). The reduced gene expression matrices were analyzed using BMDExpress 2.0 to calculate a toxicogenomic benchmark dose (BMD_t) for each treatment group (Yang et al. 2007). Here, the BMD_t was calculated as the dose that corresponded to a 10% increase in gene expression compared to the control (Farmahin et al. 2017). Within BMDExpress 2.0, genes were filtered using one-way ANOVA (FDR adjusted p-value cut-off = 0.05). A BMD_t was calculated for each differentially expressed gene by curve fitting with exponential (degree 2-5), polynomial (degree 2-3), linear, power, and Hill models. For each gene, the model with the lowest Akaike information criterion (AIC) was used to derive the BMD_t.

The BMD_ts from individual genes were used to determine a treatment group-level BMD_t using functional enrichment analysis with Reactome pathways (Farmahin et al. 2017). Note, we chose here to functionally enrich with Reactome since we utilized KEGG to derive the T1000 list. After functional enrichment analysis, significantly enriched pathways (p-value < 0.05) were filtered such that only pathways with > 3 genes and > 5% of genes in the pathway were retained. The treatment group-level BMD_t was calculated by considering the mean gene-level BMD_t for each significantly enriched pathway and selecting the lowest value. If there were no significantly enriched pathways that passed all filters, no BMD_t could be determined for that treatment group. The similarity of the BMD_t to the benchmark dose derived from apical outcomes (BMD_a) was assessed by calculating the BMD_t/BMD_a ratio and the correlation between BMD_t and BMD_a for all treatment groups (Farmahin et al. 2017). Following the same procedures, BMD_t/BMD_a ratio and correlation statistics were determined from genes belonging to L1000, S1500, and Linear Models for Microarray Data (Limma) (Smyth 2005) to provide a reference for the performance of T1000 genes.

Databases for Computing Prior Knowledge

The CTD, KEGG, and Hallmark databases were mined to integrate existing toxicogenomics and broader biological knowledge into one network that represents the prior knowledge space. CTD is manually curated from the literature to serve as a public source for toxicogenomics information, currently including over 30.5 million chemical-gene, chemical-disease, and gene-disease interactions (Davis et al. 2017). Following the recommendations of Hu et al. (2015), only “mechanistic/marker” associations were extracted from the CTD database, thus excluding “therapeutic” associations that are presumably less relevant to toxicology. The extracted subgraph contained 2,889 chemicals, 950 diseases annotated as toxic endpoints (e.g. neurotoxicity, cardiotoxicity, hepatotoxicity and nephrotoxicity), and 22,336 genes. KEGG pathways are a popular bioinformatics resource that help to link, organize, and interpret genomic information through the use of manually drawn networks describing the relationships between genes in specific biological processes (Kanehisa et al. 2007). The MSigDB Hallmark gene sets have been developed using a combination of automated approaches and expert curation to represent known biological pathways and processes while limiting redundancy (Liberzon et al. 2015b).

Each feature vector consisted of 239 dimensions, representing information encoded from Hallmark, KEGG and CTD. For the Hallmark and KEGG features, we used “1” or “0” to indicate if a gene was present or absent for each of the 50 Hallmark gene sets (Liberzon et al. 2015b) and 186 KEGG pathways (Kanehisa & Goto 2000). These features were transformed into z-scores. For the CTD features, we computed the degree, betweenness centrality, and closeness centrality of each gene, based on the topology of the extracted CTD subgraph. The topology measures were log-scaled for each gene in the network. The resulting prior knowledge space consisted of a 239-dimension vector for each of the 22,336 genes, with each vector containing 50 z-score normalized Hallmark features, 186 z-score normalized KEGG features, and three log-scaled CTD network features.

Reactome database

To understand the biological space covered by T1000, we analyzed T1000’s top enriched Reactome pathways (as KEGG was used to develop T1000). Reactome is a manually curated knowledgebase of human reactions and pathways with annotations of 7,088 protein-coding genes (Croft et al. 2014).

Performance evaluation

For the performance evaluation and testing phase, we leveraged the fourth dataset from Open TG-GATEs (see dataset 4 in **Table 1**), which was not used for gene ranking or selection so that it could serve as an external validation dataset. The dose-response dataset was used for an additional external validation (see dataset 5 in **Table 1**).

In this step, we applied five supervised machine learning methods to the TG-GATES rat kidney *in vivo* dataset, with the objective to predict which exposures caused significant "dysregulation", according to the criteria defined in step 4. This dataset was purposefully not used earlier when deriving T1000 so that it could serve later as a validation and testing dataset. The five machine learning models used were K-nearest neighbors (KNN; K = 3) (Cover & Hart 1967), Decision Trees (DT), Naïve Bayes Classifier (NBC), Quadratic Discriminant Analysis (QDA) and Random Forests (RF).

The performance of each method was evaluated with five-fold cross-validation and measured using six different metrics (Equations 2 – 7). TP represents the number of true positives, FP the number of false positives, TN the number of true negatives and FN the number of false negatives. The F_1 score (also called the balanced F-score) is a performance evaluation measure that computes the weighted average of sensitivity and precision (He & Garcia 2009), and is well-suited for binary classification models. The $F_{0.5}$ score (Davis & Goadrich 2006; Maitin-Shepard et al. 2010; Santoni et al. 2010) is another summary metric that gives twice as much weight to precision than sensitivity. The evaluation was performed on a Linux based workstation with 16 cores and 64 GB RAM for processing the data and running the experiments.

$$sensitivity = TP/(TP + FN) \qquad (1)$$

$$specificity = TN/(TN + FP) \qquad (2)$$

$$precision = TP/(TP + FP) \qquad (3)$$

$$GMean = \sqrt{sensitivity \times specificity} \qquad (4)$$

$$F_1Score = 2 \times \frac{precision \times sensitivity}{precision + sensitivity} \qquad (5)$$

$$F_{0.5}Score = 1.25 \times \frac{precision \times sensitivity}{0.25 \times precision + sensitivity} \qquad (6)$$

Proposed T1000 Framework

The work of T1000 was conducted in four discrete phases as follows (see **Figure 1**): I) data preparation and gene co-expression network generation; II) network clustering to group relevant genes; III) gene selection and prioritization; and IV) external testing and performance evaluation. The goal of phase I was to construct two network representations of the interactions between toxicologically-relevant genes, with one based on TG-GATES microarray data (step 1&2) and the other based on the KEGG, MSigDB, and CTD databases (step 3). In a co-expression network, nodes represent genes and edges represent the Pearson's correlation of expression values of pairs of genes. In the current study, we constructed three separate co-expression networks using gene expression profiles from Open TG-GATEs datasets (human *in vitro*, rat *in vitro*, and rat *in vivo*) (**Table 1**). If an interaction with a correlation coefficient of 60% or higher was present in all three networks, that gene-gene interaction was then accepted and mapped into one integrated co-expression network by averaging the absolute values of the pairwise correlation coefficients between individual genes. Matching between rat and human genes was based on gene symbols (e.g., Ddr1 in rat is matched with DDR1 in human using BiomaRt R package (Durinck et al. 2009)) and ignored when no match exists. This is a more conservative approach to maintain perfect matching orthologues in the networks although other computational approaches to match orthologues can be used (Wang et al. 2015). The final integrated co-expression network had 11,210 genes from a total of 20,502 genes.

To build the prior knowledge space (step 3), we encoded information from the Hallmark, KEGG and CTD databases into feature vectors composed of 239 features describing each gene (see Materials section). Then, we projected the data onto a two-dimensional space using principle component analysis (PCA) and clustered using K-means (K=3) to detect those genes that contributed most to the prior knowledge space. Regarding K-means, we initially experimented with K=1, K=3 and K=5 and after visual inspection of summarized information as **Supplemental Information S2 Figure 1**, we chose K=3.

Genes that were furthest from the centroids (i.e., highest contributing ones) of the K-means clusters were more enriched with pathways and gene-chemical-disease interactions (see **Supplemental Information S2**). Based on step 3, a ranked list of all genes was generated such that the first ranked gene would have a prior score of 100% and the last, a prior score close to 0%. In phase II, we re-weighted the interactions in the co-expression network based on the prior knowledge space and then detected clusters of highly connected genes in the updated network (step 4). In a Bayesian fashion, the pairwise connections between genes in the co-expression network were re-weighted by multiplying the correlation with the mean prior score. For example, given $P(A)$ and $P(B)$ as prior scores of genes A and B, the correlation score $S(A, B)$ is re-weighted as follows (Eq. 7):

$$S(A,B)_{new} = S(A,B) * ((P(A) + P(B))/2) \quad (7)$$

It should be noted that in Eq. 7, the product of joint distribution could have been considered for the update such that $S(A,B)_{new} = S(A,B) * ((P(A) * P(B))$.

After re-weighting the connections, we detected clusters of highly connected genes using the Markov Cluster Algorithm (MCL) (Van Dongen & Abreu-Goodger 2012). The MCL approach groups together nodes with strong edge weights and then simulates a random flow through a network to find more related groups of genes based on the flow's intensity of movement. It does not require the number of clusters to be pre-specified. An inflation parameter controls the granularity of the output clustering and several values within a recommended range (1.2-5.0) were tried (Van Dongen & Abreu-Goodger 2012). To optimize for the granularity of the clustering, a systematic analysis for the MCL inflation parameter was performed with values in range (1.2-5.0) (see **Supplemental Information S3**). After examining closely efficiency and mass fraction, a value of 3.3 was chosen. This generated 258 clusters that consisted of 11,210 genes. The average number of genes in each cluster was 43.4 with the min-max ranging from 1 to 8,423.

The goal of phase III of gene selection and prioritization was to select the top genes from each cluster to form T1000 (step 5), and then produce a final ranking of the 1000 selected genes (step 6). For each of the 258 gene clusters, random forest (RF) classifiers were used to rank genes based on their ability to separate changes in gene expression labelled as "dysregulated" from those labelled "non-dysregulated", using the Gini impurity index of classification (Nguyen et al. 2013; Qi 2012; Tolosi & Lengauer 2011). RF is one of the most widely used solutions for feature ranking, and as an ensemble model, it is known for its stability (Chan & Paelinckx 2008). In order to cover more biological space and ensure selected genes represent the whole transcriptome, a different RF classifier is built for each cluster and used to select representative genes (Sahu & Mishra 2012).

We selected the top genes from each cluster based on the performance of the RF classifier. For example, when selecting the 1,000 top genes from two clusters (A and B), if the cross-validation prediction accuracy estimated for models A and B were 60% and 55%, respectively, then 522 ((60%/(60%+55%))*1000) and 478 ((55%/(60%+55%))*1000) genes would be selected from clusters A and B. However, if cluster A contained only 520 genes, the remaining two genes would be taken from group B, if possible. So, the cluster size is only used if it contains insufficient genes. We repeated this process until 1000 genes were selected. After choosing top *k* genes from each cluster, we aggregated them into a single list of 1000 genes and built a final RF model to get a global ranking of the genes. We refer to this final ranked list as T1000 (see **Supplemental Table S1** for a full list of selected genes and summary annotation; see **Supplemental Information S4** for the cluster assignment of the genes). The goal of phase IV was to test the performance of the T1000 gene set using external datasets, and thus transition from gene selection activities to ones that focus on the evaluation of T1000. Phase IV is discussed in the following Results section. To discuss factors that characterizes and distinguishes T1000 from L1000 and S1500, Table 2 is provided. As summarized in Table 2, T1000 is more toxicogenomic tailored by selecting genes that optimizes for endpoint predictions and using toxicogenomic datasets. Incorporating the prior knowledge space is critical for T1000 in ranking genes with more contribution to toxic effects. L1000 aims at finding a set of genes that can be used to extrapolate for the full expression space of all other genes. S1500 has considered an optimization for the number of covered pathways. T1000, L1000 and S1500 have considered using PCA and clustering during the selection process. In T1000, however, this step is part of computing the prior only.

Results

Overview of T1000 and biological relevance

The genes comprising T1000 cover a wide biological space of toxicological relevance. For illustration, co-expression networks, before and after applying Steps 2 and 3 (i.e., networks built on the Open TG-GATEs data that are subsequently updated with prior information from KEGG, MSigDb, and CTD), are shown in **Figure 2**. In part (a) of **Figure 2**, a sample co-expression network composed of 150 genes (i.e., 150 for visualization purposes only; of the 11,210 genes identified) has, in general, similar color and size of all the nodes of the network. While this covers a broad toxicological space, it does not necessarily identify or prioritize the most important genes. After subjecting the data to steps 2 and 3, two clusters of genes with different node sizes and colors were identified (**Figure 2b**). Through this refined network, we then applied a prediction model to each cluster to identify the most representative genes resulting in the final co-expression network of the T1000 genes (**Figure 2c**).

The complete list of T1000 genes with their gene symbols and descriptions, as well as their regulation state (up- or down-regulated) is provided in **Supplemental Table S1**.

Visual examination of the Reactome enrichment map (**Supplemental Figure S2**) reveals that 'biological oxidations' (largest circle in **Supplemental Figure S2**) contained the most enriched pathways followed by 'fatty acid metabolism'. This is logical given that xenobiotic and fatty acid metabolism, mediated by cytochrome P450 (CYP450) enzymes, feature prominently across the toxicological literature (Guengerich 2007) (Hardwick 2008).

We further examine two genes that are ranked among the top up- and down-regulated gene sets, respectively. We observed that CXCL10 (ranked 2nd in up-regulated genes) and IGFALS (ranked 3rd in down-regulated genes) had reported links in the literature in response to exposure to toxic compounds. Upregulation of CXCL10, the ligand of the chemokine receptor CXCR3 found on macrophages, has been observed in the bronchiolar epithelium of patients with Chronic Obstructive Pulmonary Disease (COPD) compared to non-smokers or smokers with normal lung function (Saetta et al. 2002). Smokers develop COPD after exposure to the many chemicals found in cigarette smoke, which include oxidants that cause inflammation (Foronjy & D'Armiento 2006). Although TG-GATEs does not comprise any cigarette toxicants within its database, the general pathways by which toxicants disrupt tissue function are represented by T1000.

A gene that was found to be significantly downregulated by T1000 was the gene encoding for Insulin Like Growth Factor Binding Protein Acid Labile Subunit or IGFALS, which is an Insulin growth factor-1 (IGF-1) binding protein (Amuzie & Pestka 2010). Interestingly, the mRNA expression of IGFALS was reported to be significantly downregulated when experimental animals were fed deoxynivalenol, a mycotoxin usually found in grain (Amuzie & Pestka 2010). By reducing IGFALS, the half-life of circulating IGF-1 is reduced, causing growth retardation (Amuzie & Pestka 2010). Many compounds in the TG-GATEs database are of organismal origin, and thus, as the data suggest, they have a similar mode of action as deoxynivalenol in reducing expression of important effectors such as IGFALS.

Regarding potential clinical applications, we discuss the use of T1000 signature for screening drugs that may show toxic adverse effects in **Supplemental Information S5**. The experiment is motivated by the connectivity map project for connecting small molecules, genes, and disease using gene-expression signatures (Lamb et al. 2006).

Benchmark dose-response results

Overall, the aim of the evaluation was to assess the ability of T1000 gene sets to predict apical outcomes according to previously published methods (Farmahin et al. 2017). Additionally, we repeated step 4 of the T1000 approach to select the top 384 (T384; i.e., a number conducive to study in a QCPR microplate format as per the EcoToxChip project; (Basu et al. 2019)) and 1,500 (T1500 see **Supplemental Information S6**; i.e., a number pursued in other endeavours like S1500) genes to investigate the effect of gene set size on apical outcome prediction. To benchmark the performance of T1000 against other notable gene sets, we considered S1500 (Merrick et al. 2015) and L1000 (Subramanian et al. 2017).

BMD_t analysis (see Materials section) of the dose-response dataset was performed with the T1000 gene list and the BMDExpress software program (Yang et al. 2007). The maximum number of BMDs calculated was 21 because for three of the experimental groups a BMD_a (benchmark dose, apical outcome) did not exist due to a lack of observed toxicity (**Table 3**). The T384 gene set performed similarly with Limma; however, increasing the size of this gene set to T1000 resulted in performance evaluation metrics that rivaled that of all other gene sets of the same size or larger (L1000, Limma, and S1500). Further increasing the size of T1000 to T1500 did not increase the performance as the correlation slightly decreased while the average ratio of

BMD_t/BMD_a got slightly closer to one. **Figure 3** provides a visual summary of the comparison based on the BMD_t/BMD_a ratios.

Prediction results

In a second validation study, we applied T1000 to study the Rat Genome 230 2.0 Array for Kidney dataset from the Open TG-GATEs program. This dataset was not included in any model training or parameter tuning steps. This helped to establish another external validation of T1000 in terms of its generalized ability to predict apical outcomes for datasets derived from different tissues. When compared to baseline gene sets mapped using Limma and L1000, T1000 achieved a relative improvement of the F_1Score by 6.9% and 27.56%, respectively, thus outperforming comparison gene sets (**Table 4)**. When considering the absolute difference of F_1Score between T1000 and the second best (i.e., Limma), T1000 achieved an improvement of 1.59%. The improvement was 1.54% for $F_{0.5}$Score confirming that T1000 led to fewer false positive predictions.

Another baseline we compare with is Random-500, where a set of 1000 features are selected randomly and the performance is reported for the five classifiers considered (i.e., LDA, NBC, KNN, QDA and RF). This experiment is repeated for 500 times and the average and standard deviation scores are reported in Table 4. GMean, F1Score and F0.5Score of T1000 are significantly higher (t-test with alpha = 0.1) than the random scores. The t-test we performed was based on the average performance of the five used different machine learning (ML) classifiers. So, we averaged results of Random-500 to get a summary performance scores for each of the classifiers. One observation is that the Random-500 results outperformed several gene sets. This can be due to the fact that some machine learning models are less sensitive to the type of selected features (e.g., RF). On average, we found that a randomly generated set would outperform other models with a chance of about 30% only. Here, we focused on F0.5Measure as one of the summary performance measures. It should be noted that this does not reflect the magnitude of improvement which is measured using the t-test. Given the fact that other approaches will outperform a random selection in 70% and with a significantly higher performance on average (see T1000 in Table 4), we conclude that a systematic approach is required to prioritize genes. In the context of high throughput screening, such small improvements in F_1Score or $F_{0.5}$Score may represent large cost savings (Soufan et al. 2015a) as false positives may lead to added experiments that would otherwise be unnecessary. Detailed performance scores of each individual machine learning model are provided in **Supplemental Table S2**. Please refer to **Supplemental Information S7** for more comparisons including expression space visualization using PCA and gene set coverage evaluation.

Discussion

There is great interest across the toxicological and regulatory communities in harnessing transcriptomics data to guide and inform decision-making (Basu et al. 2019; Council 2007; ECHA 2016; Mav et al. 2018; Thomas et al. 2019). In particular, transcriptomic signatures hold great promise to identify chemical-specific response patterns, prioritize chemicals of concern, and predict quantitatively adverse outcomes of regulatory concern, in a cost-effective manner. However, the inclusion of full transcriptomic studies into standard research studies faces logistical barriers and bioinformatics challenges, and thus, there is interest in the derivation and use of reduced but equally meaningful gene sets.

Our approach to select T1000 followed the same rationale of how the LINCS program derived the L1000 dataset (Liu et al. 2015), though here we purposefully included additional steps to bolster the toxicological relevance of the resulting gene set. Generating a list of ranked genes based on toxicologically relevant input data and prior knowledge is another key feature of T1000.

There are some limitations associated with our current study. For instance, the co-expression network was based on data from the Open TG-GATEs program. While this is arguably the largest toxicogenomics resource available freely, the program is founded on one *in vivo* model (rat), two *in vitro* models (primary rat and human hepatocytes), 170 chemicals that are largely drugs, and microarray platforms. Thus, there remain questions about within- and cross- species and cell type differences, the environmental relevance of the tested chemicals, and the biological space captured by the microarray. The multi-pronged and -tiered bioinformatics approach was designed to yield a toxicologically robust gene set, and the approach can be ported to other efforts that are starting to realize large toxicogenomics databases such as our own EcoToxChip project (Basu et al. 2019). In addition, our approach in selecting T1000 genes was purely data-driven without considering input from scientific experts as was done by the NTP to derive the S1500 gene set (Mav et al. 2018). It is unclear how such gene sets (e.g., T1000, S1500) will be used by the community and under which domains of applicability, and thus there is a need to perform case studies in which new approach methods are compared to traditional methods (Kavlock et al. 2018). It worth to mention that T1000 had 259 and 90 genes in common with S1500 and L1000, respectively and 741 unique genes.

Conclusions

Here we outlined a systematic, data-driven approach to identify highly-responsive genes from toxicogenomics studies. From this, we prioritized a list of 1,000 genes termed the T1000 gene set. We demonstrated the applicability of T1000 to 7,172 expression profiles, showing great promise in future applications of this gene set to toxicological evaluations. We externally validated T1000 against two *in vivo* datasets of toxicological prominence (a kidney dataset of 308 experiments on 41 chemicals from Open TG-GATEs and a dose-response study of 30 experiments on six chemicals (Thomas et al. 2013). We compared the performance of T1000 against existing gene sets (Limma, L1000 and S1500) as well as panels of randomly selected genes. In doing so, we demonstrate T1000's versatility as it is predictive of apical outcomes across a range of conditions (e.g., *in vitro* and *in vivo*), and generally performs as well, or better than other gene sets available. Our approach represents a promising start to yield a toxicologically-relevant gene set. We hope that future efforts will start to use and apply T1000 in a diverse range of settings, and from these we can then start to make updates to the composition of the T1000 gene set based on improved understanding of its performance characteristics and user experiences.

Supplemental data

Supplemental data are available at PeerJ online.

Acknowledgements

We acknowledge the support of all members of the EcoToxChip project as well as the project's financial sponsors (Genome Canada, Génome Québec, Genome Prairie, the Government of Canada, Environment and Climate Change Canada, Ministère de l'Économie, de la Science et de l'Innovation du Québec, the University of Saskatchewan, and McGill University). We are grateful to the guidance offered by our project's program officer (Micheline Ayoub, Génome Québec) and members of our Research Oversight Committee (Chair: Nancy Denslow; Members: Kevin Crofton, Dan Schlenk, Roy Suddaby, and Carole Yauk).

Funding

This study was funded by Genome Canada, Génome Québec, Genome Prairie, the Government of Canada, Environment and Climate Change Canada, Ministère de l'Économie, de la Science et de l'Innovation du Québec, the University of Saskatchewan, and McGill University.

References

Alshahrani M, Soufan O, Magana-Mora A, and Bajic VB. 2017. DANNP: an efficient artificial neural network pruning tool. *PeerJ Computer Science* 3:e137.

Amuzie CJ, and Pestka JJ. 2010. Suppression of insulin-like growth factor acid-labile subunit expression--a novel mechanism for deoxynivalenol-induced growth retardation. *Toxicol Sci* 113:412-421. 10.1093/toxsci/kfp225

Andersen ME, and Krewski D. 2009. Toxicity testing in the 21st century: bringing the vision to life. *Toxicol Sci* 107:324-330. 10.1093/toxsci/kfn255

Basu N, Crump D, Head J, Hickey G, Hogan N, Maguire S, Xia J, and Hecker M. 2019. EcoToxChip: A next-generation toxicogenomics tool for chemical prioritization and environmental management. *Environ Toxicol Chem* 38:279-288. 10.1002/etc.4309

Budinska E, Popovici V, Tejpar S, D'Ario G, Lapique N, Sikora KO, Di Narzo AF, Yan P, Hodgson JG, Weinrich S, Bosman F, Roth A, and Delorenzi M. 2013. Gene expression patterns unveil a new level of molecular heterogeneity in colorectal cancer. *J Pathol* 231:63-76. 10.1002/path.4212

Chan JC-W, and Paelinckx D. 2008. Evaluation of Random Forest and Adaboost tree-based ensemble classification and spectral band selection for ecotope mapping using airborne hyperspectral imagery. *Remote Sensing of Environment* 112:2999-3011.

Council NR. 2007. *Toxicity testing in the 21st century: a vision and a strategy*: National Academies Press.

Cover TM, and Hart PE. 1967. Nearest neighbor pattern classification. *Information Theory, IEEE Transactions on* 13:21-27.

Croft D, Mundo AF, Haw R, Milacic M, Weiser J, Wu G, Caudy M, Garapati P, Gillespie M, Kamdar MR, Jassal B, Jupe S, Matthews L, May B, Palatnik S, Rothfels K, Shamovsky V, Song H, Williams M, Birney E, Hermjakob H, Stein L, and D'Eustachio P. 2014. The Reactome pathway knowledgebase. *Nucleic Acids Res* 42:D472-477. 10.1093/nar/gkt1102

Davis AP, Grondin CJ, Johnson RJ, Sciaky D, King BL, McMorran R, Wiegers J, Wiegers TC, and Mattingly CJ. 2017. The comparative toxicogenomics database: update 2017. *Nucleic acids research* 45:D972-D978.

Davis J, and Goadrich M. 2006. The relationship between Precision-Recall and ROC curves. Proceedings of the 23rd international conference on Machine learning: ACM. p 233-240.

Durinck S, Spellman PT, Birney E, and Huber W. 2009. Mapping identifiers for the integration of genomic datasets with the R/Bioconductor package biomaRt. *Nat Protoc* 4:1184-1191. 10.1038/nprot.2009.97

ECHA. 2007. Understanding REACH. *Available at https://echa.europa.eu/regulations/reach/understanding-reach* (accessed April 11, 2019.

ECHA. 2016. New Approach Methodologies in Regulatory Science. In: Agency EC, editor. European Chemicals Agency (ECHA). Helsinki.

Farmahin R, Williams A, Kuo B, Chepelev NL, Thomas RS, Barton-Maclaren TS, Curran IH, Nong A, Wade MG, and Yauk CL. 2017. Recommended approaches in the application of toxicogenomics to derive points of departure for chemical risk assessment. *Archives of toxicology* 91:2045-2065.

Foronjy R, and D'Armiento J. 2006. The Effect of Cigarette Smoke-derived Oxidants on the Inflammatory Response of the Lung. *Clin Appl Immunol Rev* 6:53-72. 10.1016/j.cair.2006.04.002

Gautier L, Cope L, Bolstad BM, and Irizarry RA. 2004. affy--analysis of Affymetrix GeneChip data at the probe level. *Bioinformatics* 20:307-315. 10.1093/bioinformatics/btg405

Guengerich FP. 2007. Mechanisms of cytochrome P450 substrate oxidation: MiniReview. *J Biochem Mol Toxicol* 21:163-168.

Haider S, Black MB, Parks BB, Foley B, Wetmore BA, Andersen ME, Clewell RA, Mansouri K, and McMullen PD. 2018. A Qualitative Modeling Approach for Whole Genome Prediction Using High-Throughput Toxicogenomics Data and Pathway-Based Validation. *Front Pharmacol* 9:1072. 10.3389/fphar.2018.01072

Hardwick JP. 2008. Cytochrome P450 omega hydroxylase (CYP4) function in fatty acid metabolism and metabolic diseases. *Biochem Pharmacol* 75:2263-2275. 10.1016/j.bcp.2008.03.004

He H, and Garcia EA. 2009. Learning from imbalanced data. *Knowledge and Data Engineering, IEEE Transactions on* 21:1263-1284.

Igarashi Y, Nakatsu N, Yamashita T, Ono A, Ohno Y, Urushidani T, and Yamada H. 2014a. Open TG-GATEs - Pathological items. *Available at* *https://dbarchive.biosciencedbc.jp/en/open-tggates/data-12.html*2017).

Igarashi Y, Nakatsu N, Yamashita T, Ono A, Ohno Y, Urushidani T, and Yamada H. 2014b. Open TG-GATEs: a large-scale toxicogenomics database. *Nucleic acids research* 43:D921-D927.

Irizarry RA, Bolstad BM, Collin F, Cope LM, Hobbs B, and Speed TP. 2003a. Summaries of Affymetrix GeneChip probe level data. *Nucleic acids research* 31:e15-e15.

Irizarry RA, Hobbs B, Collin F, Beazer-Barclay YD, Antonellis KJ, Scherf U, and Speed TP. 2003b. Exploration, normalization, and summaries of high density oligonucleotide array probe level data. *Biostatistics* 4:249-264. 10.1093/biostatistics/4.2.249

Kanehisa M, Araki M, Goto S, Hattori M, Hirakawa M, Itoh M, Katayama T, Kawashima S, Okuda S, and Tokimatsu T. 2007. KEGG for linking genomes to life and the environment. *Nucleic acids research* 36:D480-D484.

Kanehisa M, and Goto S. 2000. KEGG: kyoto encyclopedia of genes and genomes. *Nucleic acids research* 28:27-30.

Kavlock RJ, Bahadori T, Barton-Maclaren TS, Gwinn MR, Rasenberg M, and Thomas RS. 2018. Accelerating the Pace of Chemical Risk Assessment. *Chem Res Toxicol* 31:287-290. 10.1021/acs.chemrestox.7b00339

Knudsen TB, Keller DA, Sander M, Carney EW, Doerrer NG, Eaton DL, Fitzpatrick SC, Hastings KL, Mendrick DL, Tice RR, Watkins PB, and Whelan M. 2015. FutureTox II: in vitro data and in silico models for predictive toxicology. *Toxicol Sci* 143:256-267. 10.1093/toxsci/kfu234

Lamb J, Crawford ED, Peck D, Modell JW, Blat IC, Wrobel MJ, Lerner J, Brunet JP, Subramanian A, Ross KN, Reich M, Hieronymus H, Wei G, Armstrong SA, Haggarty SJ, Clemons PA, Wei R, Carr SA, Lander ES, and Golub TR. 2006. The Connectivity Map: using gene-expression signatures to connect small molecules, genes, and disease. *Science* 313:1929-1935. 10.1126/science.1132939

Liberzon A, Birger C, Thorvaldsdottir H, Ghandi M, Mesirov JP, and Tamayo P. 2015a. The Molecular Signatures Database (MSigDB) hallmark gene set collection. *Cell Syst* 1:417-425. 10.1016/j.cels.2015.12.004

Liberzon A, Birger C, Thorvaldsdóttir H, Ghandi M, Mesirov JP, and Tamayo P. 2015b. The molecular signatures database hallmark gene set collection. *Cell systems* 1:417-425.

Liu C, Su J, Yang F, Wei K, Ma J, and Zhou X. 2015. Compound signature detection on LINCS L1000 big data. *Mol Biosyst* 11:714-722. 10.1039/c4mb00677a

Maitin-Shepard J, Cusumano-Towner M, Lei J, and Abbeel P. 2010. Cloth grasp point detection based on multiple-view geometric cues with application to robotic towel folding. Robotics and Automation (ICRA), 2010 IEEE International Conference on: IEEE. p 2308-2315.

Mav D, Shah RR, Howard BE, Auerbach SS, Bushel PR, Collins JB, Gerhold DL, Judson RS, Karmaus AL, and Maull EA. 2018. A hybrid gene selection approach to create the S1500+ targeted gene sets for use in high-throughput transcriptomics. *PLoS One* 13:e0191105.

Merrick BA, Paules RS, and Tice RR. 2015. Intersection of toxicogenomics and high throughput screening in the Tox21 program: an NIEHS perspective. *International journal of biotechnology* 14:7-27.

Necsulea A, Soumillon M, Warnefors M, Liechti A, Daish T, Zeller U, Baker JC, Grutzner F, and Kaessmann H. 2014. The evolution of lncRNA repertoires and expression patterns in tetrapods. *Nature* 505:635-640. 10.1038/nature12943

Nguyen C, Wang Y, and Nguyen HN. 2013. Random forest classifier combined with feature selection for breast cancer diagnosis and prognostic. *Journal of Biomedical Science and Engineering* 6:551.

Qi Y. 2012. Random forest for bioinformatics. *Ensemble machine learning*: Springer, 307-323.

Saetta M, Mariani M, Panina-Bordignon P, Turato G, Buonsanti C, Baraldo S, Bellettato CM, Papi A, Corbetta L, Zuin R, Sinigaglia F, and Fabbri LM. 2002. Increased expression of the chemokine receptor CXCR3 and its ligand CXCL10 in peripheral airways of smokers with chronic obstructive pulmonary disease. *Am J Respir Crit Care Med* 165:1404-1409.

Sahu B, and Mishra D. 2012. A novel feature selection algorithm using particle swarm optimization for cancer microarray data. *Procedia Engineering* 38:27-31.

Santoni FA, Hartley O, and Luban J. 2010. Deciphering the code for retroviral integration target site selection. *PLoS computational biology* 6:e1001008.

Smyth GK. 2005. Limma: linear models for microarray data. *Bioinformatics and computational biology solutions using R and Bioconductor*: Springer, 397-420.

Soufan O, Ba-alawi W, Afeef M, Essack M, Rodionov V, Kalnis P, and Bajic VB. 2015a. Mining Chemical Activity Status from High-Throughput Screening Assays. *PLoS One* 10:e0144426. 10.1371/journal.pone.0144426

Soufan O, Kleftogiannis D, Kalnis P, and Bajic VB. 2015b. DWFS: a wrapper feature selection tool based on a parallel genetic algorithm. *PLoS One* 10:e0117988. 10.1371/journal.pone.0117988

Subramanian A, Narayan R, Corsello SM, Peck DD, Natoli TE, Lu X, Gould J, Davis JF, Tubelli AA, Asiedu JK, Lahr DL, Hirschman JE, Liu Z, Donahue M, Julian B, Khan M, Wadden D, Smith IC, Lam D, Liberzon A, Toder C, Bagul M, Orzechowski M, Enache OM, Piccioni F, Johnson SA, Lyons NJ, Berger AH, Shamji AF, Brooks AN, Vrcic A, Flynn C, Rosains J, Takeda DY, Hu R, Davison D, Lamb J, Ardlie K, Hogstrom L, Greenside P, Gray NS, Clemons PA, Silver S, Wu X, Zhao WN, Read-Button W, Wu X, Haggarty SJ, Ronco LV, Boehm JS, Schreiber SL, Doench JG, Bittker JA, Root DE, Wong B, and Golub TR. 2017. A Next Generation Connectivity Map: L1000 Platform and the First 1,000,000 Profiles. *Cell* 171:1437-1452 e1417. 10.1016/j.cell.2017.10.049

Thomas RS, Bahadori T, Buckley TJ, Cowden J, Deisenroth C, Dionisio KL, Frithsen JB, Grulke CM, Gwinn MR, Singh A, Richard AM, Williams AJ, Deisenroth C, Grulke CM, Patlewicz G, Shah I, Cowden J, Wambaugh JF, Harrill JA, Paul-Friedman K, Houck KA, Gwinn MR, Linnenbrink M, Setzer RW, Sams R, Judson RS, Simmons SO, Knudsen TB, Thomas RS, Lambert JC, Bahadori T, Swank A, Wetmore BA, Ulrich EM, Sobus JR, Phillips KA, Dionisio KL, Isaacs KK, Strynar M, Tornero-Valez R, Newton SR, Buckley TJ, Frithsen JB, Villeneuve DL, Hunter ES, III, Simmons JE, Higuchi M, Hughes MF, Padilla S, Shafer TJ, and Martin TM. 2019. The next generation blueprint of computational toxicology at the U.S. Environmental Protection Agency. 10.1093/toxsci/kfz058

Thomas RS, Wesselkamper SC, Wang NCY, Zhao QJ, Petersen DD, Lambert JC, Cote I, Yang L, Healy E, and Black MB. 2013. Temporal concordance between apical and transcriptional points of departure for chemical risk assessment. *toxicological sciences* 134:180-194.

Tolosi L, and Lengauer T. 2011. Classification with correlated features: unreliability of feature ranking and solutions. *Bioinformatics* 27:1986-1994. 10.1093/bioinformatics/btr300

van Dam S, Vosa U, van der Graaf A, Franke L, and de Magalhaes JP. 2018. Gene co-expression analysis for functional classification and gene-disease predictions. *Brief Bioinform* 19:575-592. 10.1093/bib/bbw139

Van Dongen S, and Abreu-Goodger C. 2012. Using MCL to extract clusters from networks. *Bacterial Molecular Networks*: Springer, 281-295.

Villeneuve DL, and Garcia-Reyero N. 2011. Vision & strategy: Predictive ecotoxicology in the 21st century. *Environ Toxicol Chem* 30:1-8. 10.1002/etc.396

Wang Y, Coleman-Derr D, Chen G, and Gu YQ. 2015. OrthoVenn: a web server for genome wide comparison and annotation of orthologous clusters across multiple species. *Nucleic Acids Res* 43:W78-84. 10.1093/nar/gkv487

Yang L, Allen BC, and Thomas RS. 2007. BMDExpress: a software tool for the benchmark dose analyses of genomic data. *BMC genomics* 8:387.

Figure 1

Framework of the T1000 approach for gene selection and prioritization.

Phase I is composed of Steps [1-3]. After data is prepared in Step 1, the co-expression network is generated through Step 2. The prior knowledge scores are computed using (KEGG, MSigDB) and toxicological (CTD) relevance graphs in Step 3. Phase II involves Step 4 for re-weighting of the co-expression scores based on prior knowledge of biological and toxicological relevance graphs. In addition, the graph is clustered during Step 4. In Phase III, in Step 5, a prediction model is trained for each cluster. Then, after selecting top genes from each cluster in Step 5, a one final prediction model called global is trained to rank all selected genes (Step 6). Phase IV is a focused on external evaluation of the prioritized gene list.

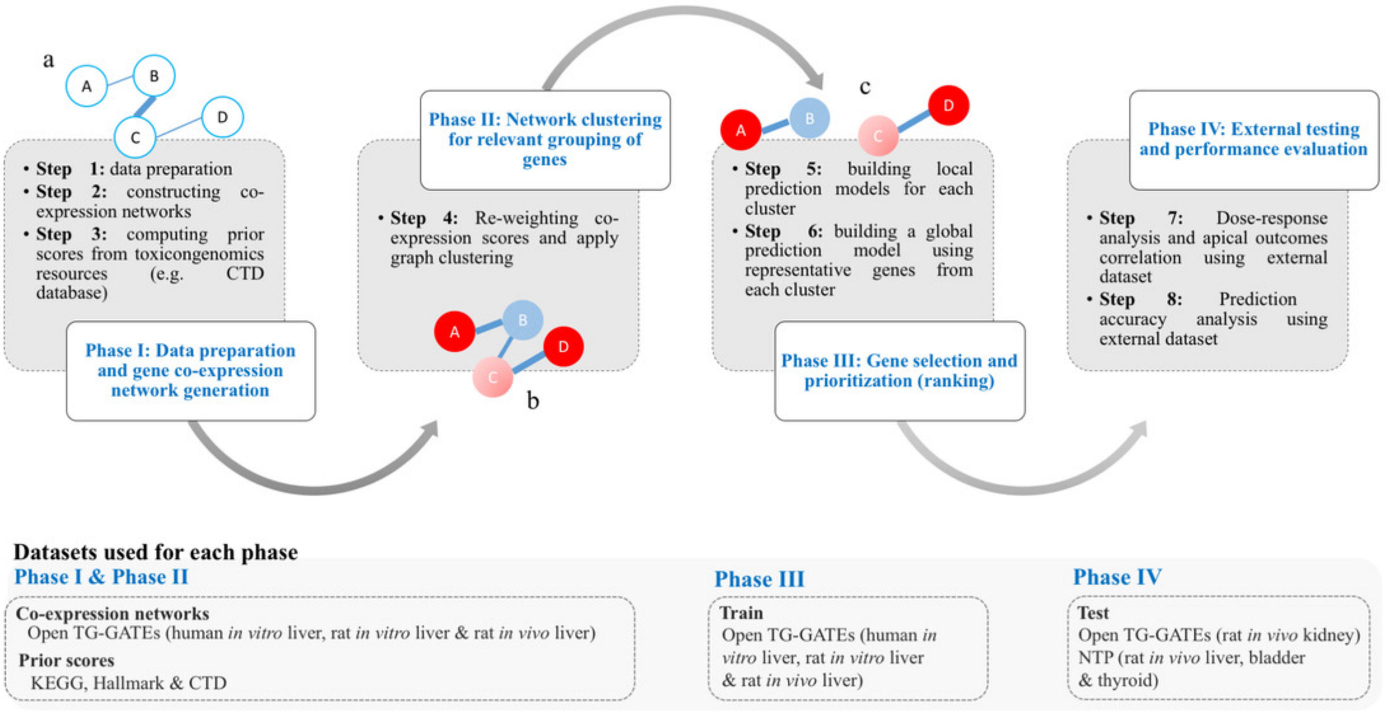
a
A
B
C
D
• Step 1: data preparation
• Step 2: constructing co-expression networks
• Step 3: computing prior scores from toxicongenomics resources (e.g. CTD database)
Phase I: Data preparation and gene co-expression network generation
Phase II: Network clustering for relevant grouping of genes
• Step 4: Re-weighting co-expression scores and apply graph clustering
A
B
C
D
b
c
A
B
C
D
• Step 5: building local prediction models for each cluster
• Step 6: building a global prediction model using representative genes from each cluster
Phase III: Gene selection and prioritization (ranking)
Phase IV: External testing and performance evaluation
• Step 7: Dose-response analysis and apical outcomes correlation using external dataset
• Step 8: Prediction accuracy analysis using external dataset
Datasets used for each phase
Phase I & Phase II
Co-expression networks
Open TG-GATEs (human in vitro liver, rat in vitro liver & rat in vivo liver)
Prior scores
KEGG, Hallmark & CTD
Phase III
Train
Open TG-GATEs (human in vitro liver, rat in vitro liver & rat in vivo liver)
Phase IV
Test
Open TG-GATEs (rat in vivo kidney)
NTP (rat in vivo liver, bladder & thyroid)

Figure 2

Visual representation of co-expression networks before and after performing Steps 2 and 3 of the T1000 selection process.

Visual representation of co-expression networks before and after performing Steps 2 and 3 of the T1000 selection process. A sample co-expression network of a group of 150 genes such that each pair of genes would have a connection is provided in Part (a). After re-weighting the correlation scores using the prior knowledge of biological and toxicological relevance graphs and performing clustering through Steps [1-4] of T1000 framework (see Figure 1), the graph in Part (a) is evolved to the one in Part (b). In Part (b), a pair of genes would have a link only if they hold enough confidence after applying prior scores. From part (b), nodes representing genes gain different levels of colors summarizing different levels of structural representations in the graph. Therefore, it is more relevant to cluster the graph at this stage after applying prior weights instead of the stage of Part (a). We can visually detect two separate clusters of genes in Part (b). After executing T1000 framework, we visualize the generated co-expression graph of all selected 1000 genes in Part (c). Compared to Part (a), we see variant levels of colors indicating different structural relevance. The colors in Parts (a), (b), and (c) reflect structural statistics using betweenness centrality and node degree. Part (a) holds a very similar statistics while Parts (b), (c) exploits and shows variant levels. A more contributing gene would have a larger node and a darker blue color while a less important one would have a very small node with a red color intensity. Please note that Parts (b) and (c) are realized only after executing steps from T1000 framework while Part (a) shows the generic representation of the co-expression graph.

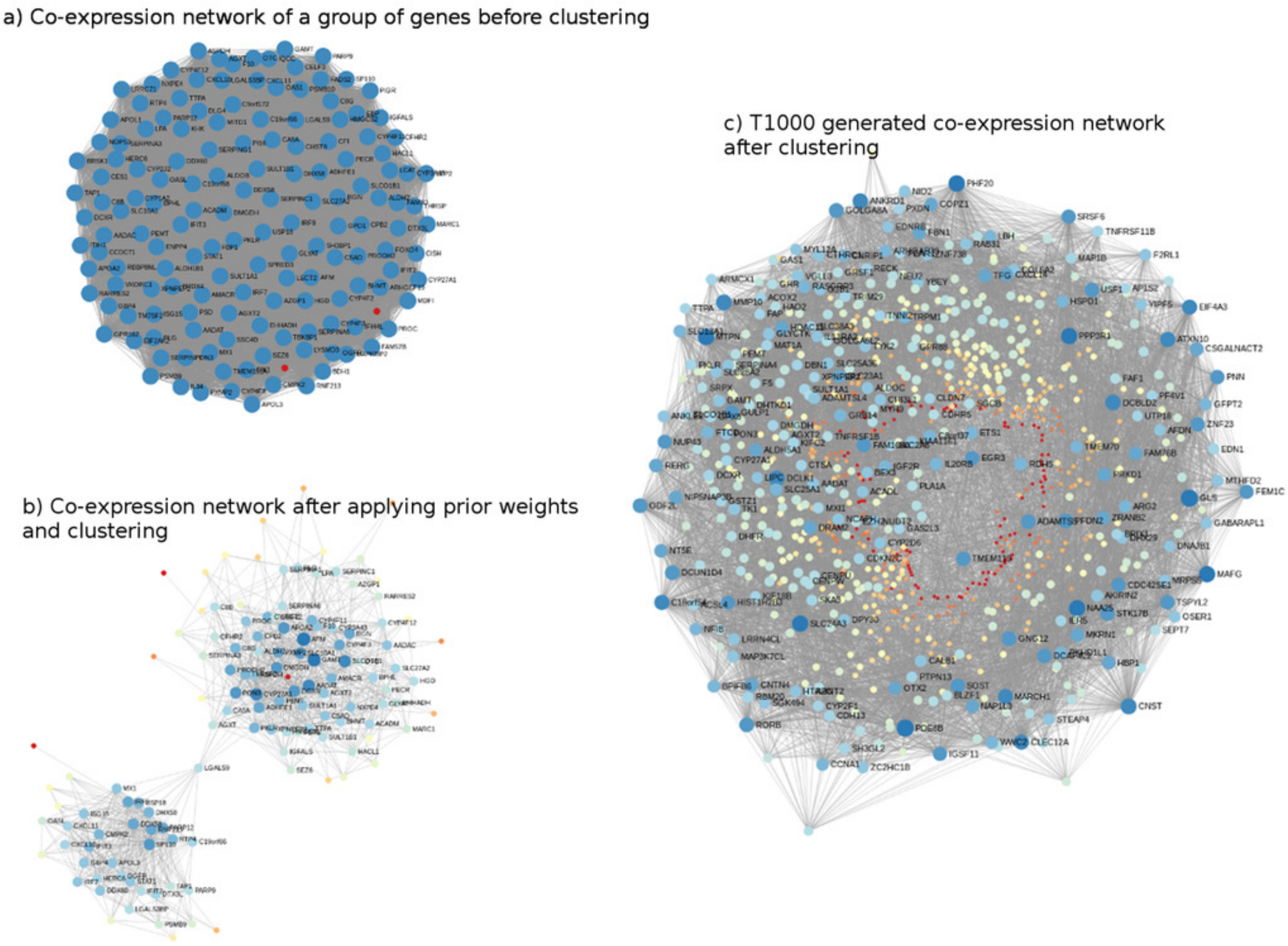

a) Co-expression network of a group of genes before clustering
b) Co-expression network after applying prior weights and clustering
c) T1000 generated co-expression network after clustering
PHF20
ANKRD1
GOLGA8A
COPZ1
SRSF6
TNFRSF11B
F2RL1
EIF4A3
CSGALNACT2
PNN
GFPT2
ZNF23
EDN1
MTHFD2
FEM1C
GABARAPL1
DNAJB1
MAFG
TSPYL2
OSER1
SEPT7
HBP1
CNST
CLEC12A
IGSF11
ZC2HC1B
CCNA1
SH3GL2
RORB
PDE6B
BPIFB6
NT5E
DCUN1D4
ODF2L
NUP43
TTPA
ARMCX1
MMP10
PPP3R1
STEAP4
ATXN10
LGALS9
IGFALS
SEZ6
MX1
PSMB9
C19orf66

Figure 3

Ratios of BMDt/BMDa for each experimental group determined with various gene sets as indicated atop the plots.

Ratios of BMDt/BMDa represents ratio of transcriptionally-derived benchmark doses BMDt using gene signatures to apical outcome-derived benchmark dose BMDa serving as the ground truth. The limits of the blue rectangular band and dotted lines represent 3-fold and 10-fold of unity, respectively. Ratios could not be calculated for three experimental groups (hydrazobenzene (HZBZ): 5 day, 2 week, 4 week) due to a lack of apical outcomes. Red circles represent mean ratios greater than 10-fold, while the yellow ones represent ratios greater than 3-fold. The fewer circles, the more the gene set is indicative of potential relevance to the examined apical endpoints (see Supplementary Figure 3 and 4 for T384 and T1500 plots, respectively). In Part a), the T1000 results are highlighted such that in only two experiments, the ratio of difference from the ground truth was greater than 3 folds and less than 10. In Parts b,c&d, the results of L1000, S1500 and Limma are illustrated, respectively, with each having a single experiment (i.e., red circle) with 10-fold difference from the ground truth. All of them had more yellow circles as compared to Part a of T1000.

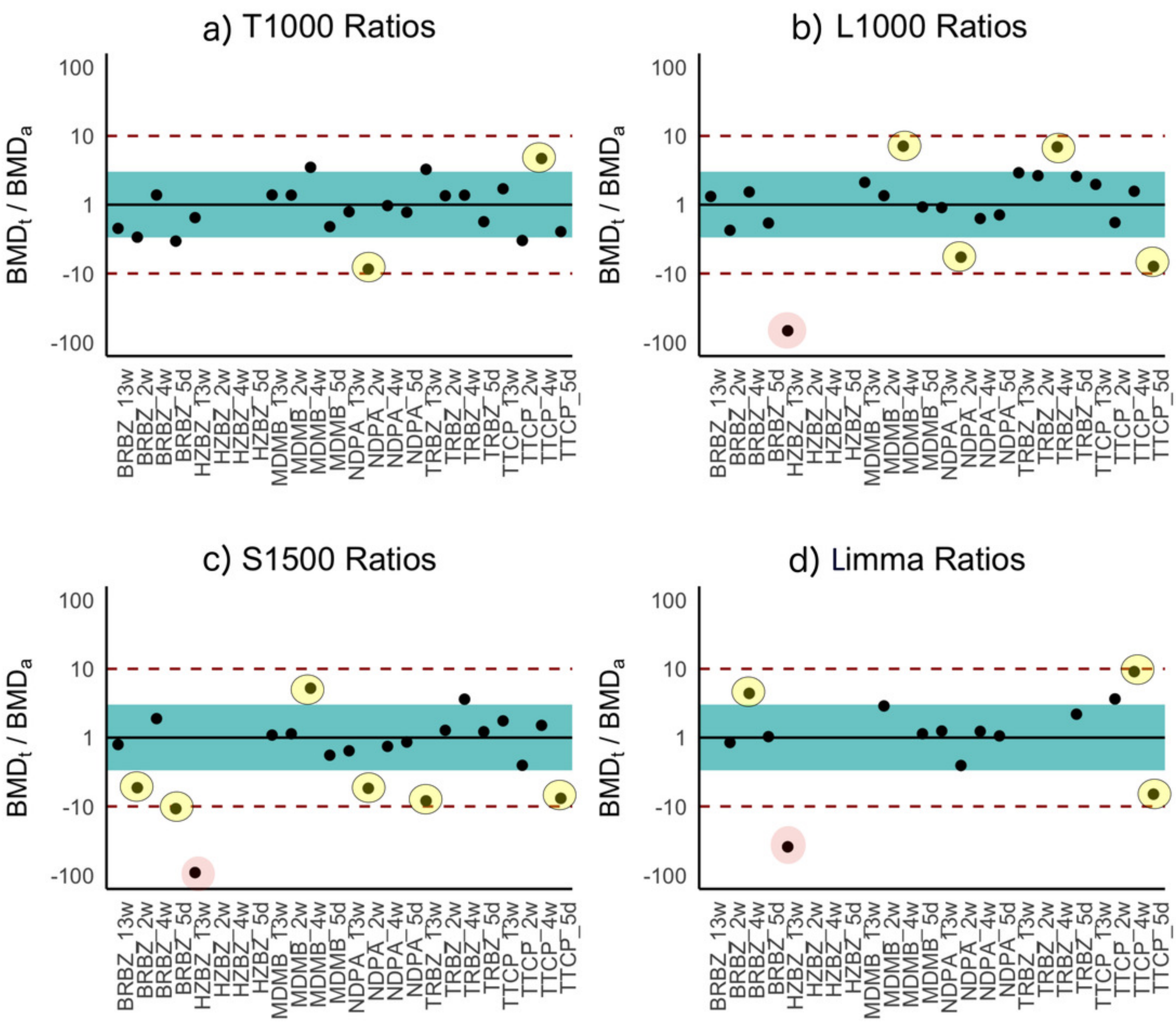
a) T1000 Ratios
b) L1000 Ratios
c) S1500 Ratios
d) Limma Ratios
BMD_t / BMD_a
100
10
1
-10
-100
BRBZ_13w
BRBZ_2w
BRBZ_4w
BRBZ_5d
HZBZ_13w
HZBZ_2w
HZBZ_4w
HZBZ_5d
MDMB_13w
MDMB_2w
MDMB_4w
MDMB_5d
NDPA_13w
NDPA_2w
NDPA_4w
NDPA_5d
TRBZ_13w
TRBZ_2w
TRBZ_4w
TRBZ_5d
TTCP_13w
TTCP_2w
TTCP_4w
TTCP_5d

Table 1(on next page)

Summary of datasets used in the current study.

Datasets 1-3 were used to develop T1000 (see Phase I, II & III in Methods Section) and datasets 4 and 5 (see Phase IV in Methods Section) were used to evaluate the performance of the gene sets.

Dataset #	**Dataset**	**Organism**	**Organ**	**Exposure Type**	**Number of chemicals**	**Matrix size (% missing values)**	**Purpose in Current Study**
1	Open TG-GATEs	Human	Liver	*in vitro*	158 chemicals	2,606 experiments x 20,502 genes (8.9%)	Training
2	Open TG-GATEs	Rat	Liver	*in vitro*	145 chemicals	3,371 experiments x 14,468 genes (11.6%)	Training
3	Open TG-GATEs	Rat	Liver	*in vivo* (single dose)	158 chemicals	857 experiments x 14,400 genes (11.5%)	Training
4	Open TG-GATEs	Rat	Kidney	*in vivo* (single dose)	41 chemicals	308 experiments x 14,400 genes (12.2%)	Testing
5	Dose-response (GSE45892)	Rat	Liver, Bladder, Thyroid	*in vivo* (repeated dose)	6 chemicals	30 experiments x 14,400 genes (0%)	Testing (external validation)
Total						7,172 experiments	

Table 2(on next page)

Descriptive comparison of T1000 against existing gene sets.

For the ‘selection criteria’ column, expression space coverage refers to the goal of finding a subset of genes that would achieve high correlation with the original full set of genes.Pathway coverage refers to finding a subset of genes that cover more pathways in a reference library.

Gene set	Selection criteria	Ranked gene list	Species	Data	Approach	Number of genes
L1000	Expression space coverage	No	Human	L1000 data	PCA and clustering (Data mining)	978
S1500 (NTP 2018)	Pathway coverage that combines data-driven and knowledge-driven activities	No	Human	Public GEO expression datasets (mainly GEO 3339 gene expression series)	PCA, clustering, and other data-driven steps (Data mining)	2861 (includes L1000 genes)
T1000	Toxicological relevance using endpoint prediction	Yes	Human and Rat	Open TG-GATEs that is founded on co-expression networks from CTD, KEGG and Hallmark	Co-expression network and prior knowledge (Graph mining). PCA and clustering are used only for the prior knowledge.	1000

Table 3(on next page)

Summary of correlation of apical endpoints to 24 experimental groups (6 chemicals x 4 exposure durations).

	T384 (n = 384)	**T1000 (n = 1000)**	**T1500 (n = 1500)**	**L1000 (n = 976)**	**S1500 (n = 2861)**	**Limma (n = 1000)**
# of BMD$_t$s	18	21	21	21	21	14
Mean ratio (BMD$_t$/BMD$_a$)	2.2	1.2	1.1	1.8	1.1	2.1
Correlation (BMD$_t$, BMD$_a$)	0.83 ($p <$ 0.001)	**0.89** ($p <$ 0.001)	0.83 ($p <$ 0.001)	0.76 ($p <$ 0.001)	0.78 ($p <$ 0.001)	0.73 ($p < 0.01$)

Table 4(on next page)

Summary comparison of average classification performance using the testing RatKidney dataset. Scores are based on average results from five classifiers (LDA, NBC, QDA, DT and RF) and the standard deviation is reported to highlight variance of estimate.

*Statistically significant at an alpha level of 0.1 using T-test and considering comparison with Random results.

	Sensitivity	Specificity	Precision	Gmean	F1Measure	F0.5Measure
T1000	**29.25% (±11.64)***	71.33% (±4.74)	**21.51% (±4.45)**	**44.7% (±7.8)***	**24.58% (±7.11)***	**22.6% (±5.36)**
Limma	27.76% (±16.3)	70.75% (±6.33)	20% (±9.96)	41.84% (±14.81)	22.99% (±12.04)	21.06% (±10.64)
CD	21.79% (±15.39)	68.08% (±10.97)	13.94% (±6.64)	34.79% (±13.3)	16.65% (±9.96)	14.83% (±7.82)
L1000	22.99% (±12.82)	70.42% (±5.78)	16.84% (±7.29)	38.33% (±11.46)	19.27% (±9.27)	17.71% (±7.97)
S1500	21.79% (±7.65)	**72.67% (±3.98)***	17.87% (±3.99)	39.19% (±6.2)	19.53% (±5.42)	18.48% (±4.48)
Random-500	27.83% (±11.69)	70.89% (±5.09)	20.31% (±4.89)	42.81% (±8.38)	18.41% (±12.03)	21.29% (±5.79)
P-value (T1000 vs. Random)	0.0555	0.3454	0.1283	0.0504	0.0192	0.1112
Best Model (Limma_NBC)	44.78%	68.75%	28.57%	55.48%	34.88%	30.80%
Worst Model (Limma_QDA)	4.48%	72.08%	4.29%	17.97%	4.38%	4.32%